

# Evaluation of increased subchondral bone density in areas of contact in the metacarpophalangeal joint during joint loading in horses

Katrina L. Easton, BS, and Chris E. Kawcak, DVM, PhD

**Objective**—To quantitatively evaluate contact area under 2 loads and subjectively compare contact areas with subchondral bone (SCB) density patterns in intact metacarpophalangeal joints of horses.

**Sample Population**—6 forelimbs from horses without musculoskeletal disease.

**Procedures**—Computed tomographic scans of intact metacarpophalangeal joints were analyzed to obtain SCB density measurements. Each limb was loaded on a materials testing system to 150° and 120° extension in the metacarpophalangeal joint, and the joint was stained via intra-articular injection with safranin-O or toluidine blue, respectively. Each joint was disarticulated, and the surface area was digitized. Total articular surface area, contact area, and percentage contact area at each angle were calculated for the distal third metacarpal condyles, the proximal phalanx, and the proximal sesamoid bones.

**Results**—Contact area on the third metacarpal condyles, proximal sesamoid bones, and the proximal phalanx significantly increased with increased load. Areas of contact subjectively appeared to have a higher density on computed tomographic scans.

**Conclusions and Clinical Relevance**—Areas consistently in contact under higher load were associated with increased SCB density. This supports the idea that the SCB adapts to the load applied to it. As load increased, contact area also increased, suggesting that areas not normally loaded may have a high degree of stress during impact loading. Quantifying how contact in the joint changes under different loading conditions and the adaptation of the bone to this change in normal and abnormal joints may provide insight into the pathogenesis of osteochondral disease. (*Am J Vet Res* 2007;68:816–821)

Joint disease in horses is naturally occurring and rapidly progressive and a major cause of lameness and retirement in horses.<sup>1</sup> It is of great concern to equine practitioners, especially those who work with equine athletes. The MCP of racehorses is especially susceptible to a wide variety of injuries, including osteochondral fragmentation, fracture, and SCB necrosis, which can lead to osteoarthritis and even catastrophic failure. Studies in the United States<sup>2,3</sup> and the United Kingdom<sup>4</sup> examining racing fatalities found that fractures of the proximal sesamoid bones and MC III were the most frequent sites of fracture and the most common catastrophic injuries.

Osteoarthritis can be the end result of traumatic injuries or repeated cyclic fatigue common in competitive events.<sup>5,6</sup> Chronic cyclic loading can lead to abnormal bone adaptation that results in sclerotic or necrotic bone as well as articular cartilage thinning. This fatigue damage can weaken the bone such that it is less able to withstand the stress associated with racing or even everyday life. Eckstein et al<sup>7</sup> determined that SCB density

ABBREVIATIONS	
MCP	Metacarpophalangeal joint
SCB	Subchondral bone
MC III	Third metacarpal bone
CT	Computed tomography
MRI	Magnetic resonance imaging

is a reflection of the loading history of the overlying articular surfaces. It would follow, therefore, that how the bones within a joint contact each other and how that contact changes with varying loads would play an important role in determining SCB adaptation and density patterns. Various studies have revealed changes in contact area in the MCP as load was increased. Colahan et al<sup>8</sup> used pressure film to detect increasing compression and contact area in the MCP as the joint was extended. However, only trends were presented and no absolute values were given. Brama et al<sup>9</sup> used a methylene blue staining technique to determine a positive correlation between contact area of the proximal phalanx and applied load. In addition, under increasing load, areas of the dorsal articular margin not normally loaded in the standing or walking horse had the highest peak pressures. Results of these studies<sup>8,9</sup> suggest that the site and type of injury may be related to how the joint surfaces articulate and how the contact area changes under increasing load. However, in the first study,<sup>8</sup> the integrity of the joint had to be disrupted for the pressure film to

Received October 21, 2006.

Accepted February 15, 2007.

From the Department of Clinical Sciences, College of Veterinary Medicine and Biomedical Sciences, Colorado State University, Fort Collins, CO 80523.

Supported by the Equine Orthopaedic Research Laboratory, Department of Clinical Sciences, Colorado State University.

Address correspondence to Dr. Kawcak.

be inserted. Although the joint was intact in the second study,<sup>9</sup> the authors only reported values for the proximal phalanx. They also only used 1 stain and therefore were only able to calculate contact area for 1 applied load/limb. To the authors' knowledge, no studies have been performed to investigate change in contact area in the MCP as a whole and within a single limb and correlate it to the SCB density pattern.

The first objective of this study, therefore, was to quantitatively evaluate change in contact area under 2 loads (standing and the stance phase of gallop) by use of a unique toluidine blue and safranin-O dual staining technique. The second objective was to subjectively compare contact area patterns with SCB density patterns to determine whether it would be beneficial to quantitatively investigate this correlation in future studies. It was hypothesized that the percentage of contact area would increase with increasing load and that areas of high SCB density would be correlated with areas of contact, especially those areas under contact at high loads.

### Materials and Methods

Six forelimbs were obtained from horses evaluated at the necropsy service in the Diagnostic Laboratory at the Veterinary Medical Center at Colorado State University for nonmusculoskeletal diseases. Only 6 limbs were used because this was a proof-of-principle study concentrating on the development of the dye staining protocol and its possible future use to study various influences on skeletal adaptation. No demographic data were collected; therefore, no inferences as to the effect of age, breed, sex, or use were made. The limbs were removed at the shoulder joint, and the humerus of each limb was cut transversely just distal to the deltoid tuberosity. The muscle and bone not covered with skin were wrapped in saline (0.9% NaCl) solution-soaked gauze, and the limbs were double bagged and stored at -20°C until testing. The limbs were thawed at room temperature (22°C) for 36 hours prior to testing.

**CT scans**—Computed tomographic scans of the intact MCP joints were performed on 5 of the limbs prior to testing. For the sixth sample, a CT scan of the distal condyle of MC III was performed after testing and disarticulation of the joint. Results of another study<sup>8</sup> indicate that bone density is not influenced by CT scanning of intact versus disarticulated limbs; therefore, having the CT scan on the sixth sample after disarticulation should not have affected the SCB density pattern, which was only used for subjective analysis. The scans

were performed with a commercially available scanner<sup>b</sup> at 130 kV and 150 mA, with 1.5-mm slice thickness and transverse slice orientation. The raw CT data were imported into a custom written analysis program<sup>a,c,d</sup> that allows for density measurements and 3-dimensional image rendering of the slices.

**Dye staining**—The humerus and hoof were potted in customized molds by use of a 2-part plastic material.<sup>e</sup> The humerus was placed in a specially designed jig that mounts to the actuator of a materials testing system,<sup>f</sup> and the hoof was placed in a specially designed jig that mounts to the load cell platen of the materials testing system. The limbs were loaded on the materials testing system until the angle (measured with a goniometer) between MC III and the proximal phalanx was 150°. McGuigan and Wilson<sup>10</sup> determined that the angle in the MCP during the stance phase of walking is 144°. The 150° angle was chosen to roughly estimate the MCP angle during the stance-stance phase of walking. By use of 18-gauge × 1.5-inch needles in 5 locations, a 1:1,000 safranin-O solution was injected into the MCP until additional distention was difficult (approx 60 mL). The safranin-O solution was allowed to remain in the joint for 2 minutes; then the joint was flushed with saline solution until the solution ran clear. The angle was measured again after the procedure to ensure that the angle had not changed during the staining process. The process was repeated in the same limb at 120° extension, which is roughly equivalent to the stance phase

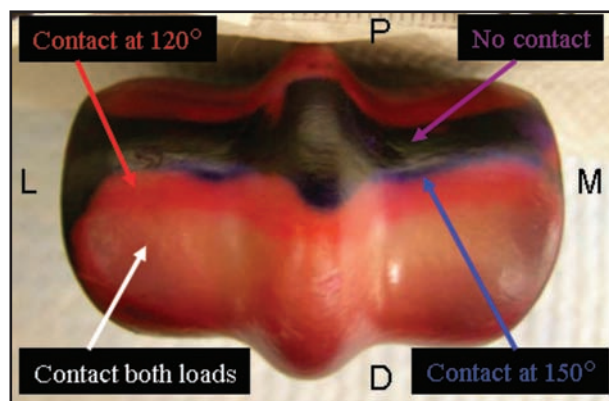


Figure 1—Photograph of the distal condyle of MC III of a horse, illustrating areas of articular cartilage contact. Blue-stained areas represent contact at 150° but not 120°. Red-stained areas represent contact at 120° but not 150°. Purple-stained areas represent areas where there was no contact at either angle. White areas represent areas where there was contact at both angles. L = Lateral. M = Medial. D = Dorsal. P = Palmar.

Table 1—Mean ± SD percentage values for contact area in various locations in MCPs of 6 equine forelimbs at angles of 150° and 120°.

Anatomic location	150°	120°	P value	Ratio of variance
Distal condyle MC III	56 ± 9.2	76 ± 1.8	0.002	0.035*
Lateral proximal sesamoid	55 ± 6.2	100 ± 0	< 0.001	0*
Medial proximal sesamoid	51 ± 10	100 ± 0	< 0.001	0*
Proximal phalanx	67 ± 13	87 ± 6.6	0.01	0.243

*P* value indicates comparison between contact areas at 150° and 120°.  
\*Ratio of variance for 120° versus 150° (variance<sub>120°</sub>/variance<sub>150°</sub>) is significantly (*P* < 0.05) different from 1.

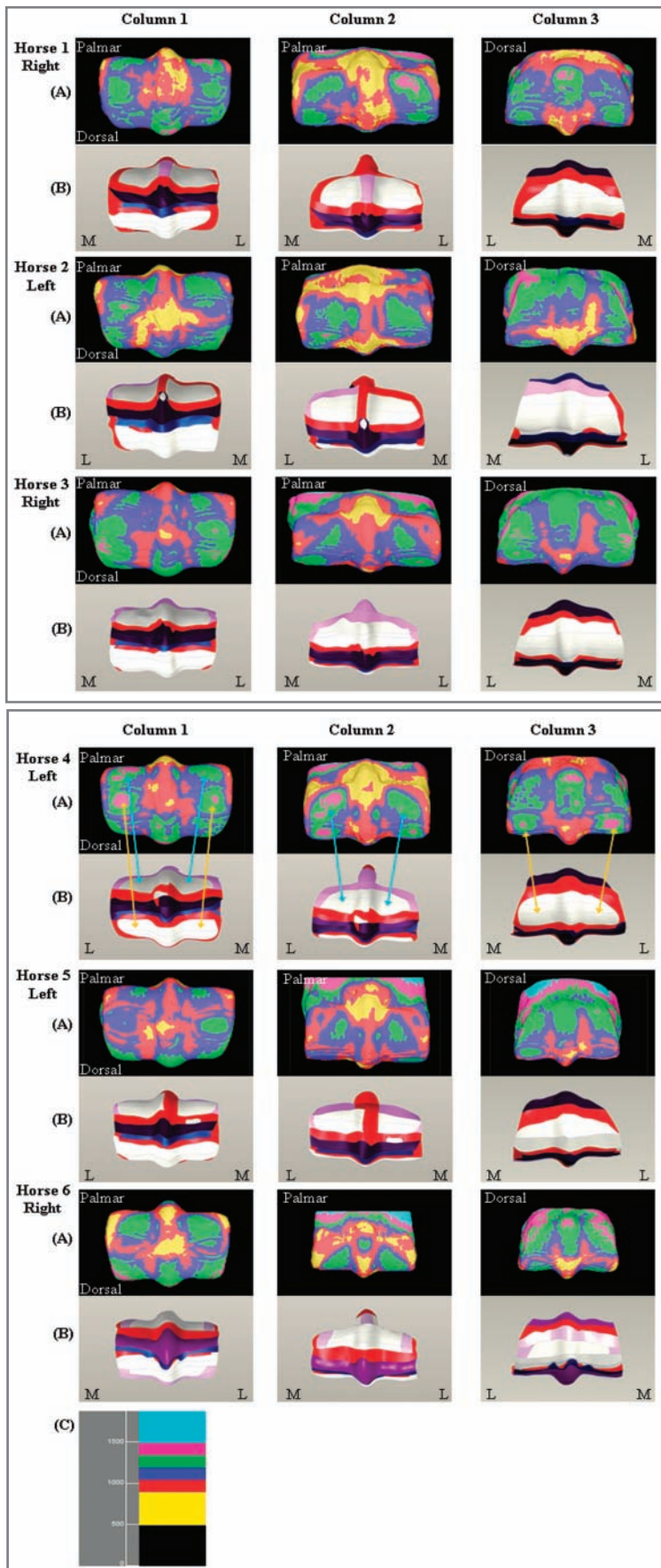


Figure 2—Comparison of CT scans and models of MC III in 6 horses used to determine the increase in SCB density in areas of high contact. Column 1 = Distal surface of the distal condyle of MC III. Column 2 = Palmar surface of the distal condyle of MC III. Column 3 = Dorsal surface of the distal condyle of MC III. Row A = Three-dimensional rendering of CT scan of the distal condyle of MC III revealing the SCB density pattern. Row B = Three-dimensional computer model revealing contact area (white = contact at both 150° and 120°; blue = contact at 150° but not 120°; red = contact at 120° but not 150°; purple = no contact at either angle; pink = diffuse staining). Row C = Reference color scale for CT data. Numbers are in Hounsfield units. Increasing numbers correspond to increasing density. Blue arrows on images of horse 4 indicate where the proximal sesamoid bones were in contact with the distal condyle of MC III. This corresponded to higher density, as indicated by the pink and green areas on the CT scan. Yellow arrows indicate where the proximal phalanx was in contact with the distal condyle of MC III; notice that the corresponding density gradient is increased in this area.

during galloping,<sup>10</sup> and the joint was infused with a 1:1,000 toluidine blue solution for 1 minute. Results of a pilot study indicated that these staining times provided the best contrast between colors (2 minutes' staining with toluidine blue resulted in the stain being too dark). Because the force required to obtain consistent angles would vary on the basis of the size of the horse and compliance of the limb, angle measurement was used instead of force to position the joint. The force required to obtain these angles was not recorded. After the saline solution flush, the joint was disarticulated and rinsed thoroughly with water. These 2 stains were chosen because they bind the sulfated glycosaminoglycan in the matrix of the articular cartilage and are commonly used to evaluate cartilage histologically. The disarticulated joint was observed for any gross abnormalities. The distal condyle of MC III, proximal sesamoid bones, and proximal phalanx were removed, double wrapped in plastic wrap, placed in a bag, and stored at -20°C until further analysis. To minimize any possible running of the dye, specimens were not wrapped in saline solution-soaked gauze. The contact between the articular surfaces of the bone was sufficient to preclude dye from these areas; therefore, white areas on the articular surface corresponded to areas where there was contact at both loads. Toluidine blue-stained areas (blue) represented contact at 150°, but not 120°. Safranin-O-stained areas (red) represented contact at 120°, but not 150°, and a combination of the 2 stains, purple-stained areas, represented areas that made no contact at either angle (Figure 1).

**Model rendering and analysis**—The total articular surface area of the distal condyle of MC III and the areas of articular contact were digitized and rendered into a 3-dimensional computer model by use of a 3-dimensional coordinate measurement system<sup>11,g</sup> and computer-aided design software.<sup>12,h</sup> Total

articular surface area, area in contact at each angle, and percentage area in contact at each angle were calculated for the distal condyle of MC III, proximal phalanx, and proximal sesamoid bones. Percentage contact area was compared between the 2 loads by use of a paired *t* test; a value of  $P < 0.05$  was considered significant. Because results of previous studies<sup>7</sup> indicate that the SCB density is a reflection of the loading history, it would follow that areas with contact under high loads would be associated with areas of higher density. To test this hypothesis, the 3-dimensional computer model revealing the contact area was subjectively compared with the CT scan that revealed the SCB density pattern. Because this was a subjective evaluation, only gross comparisons are reported here.

## Results

The stains were readily distinguishable (Figure 1), no change in the angle before and after the staining procedure was measured, and no gross abnormalities were observed. A significant increase in contact area on the condyle of MC III, proximal sesamoid bones, and proximal phalanx was found (Table 1). The proximal sesamoid bones and intersesamoidean ligament accounted for  $42 \pm 7.9\%$  of the contact on the condyle of MC III at  $150^\circ$  and  $46 \pm 1.4\%$  at  $120^\circ$ . The proximal phalanx accounted for  $57 \pm 7.9\%$  of the contact on the condyle of MC III at  $150^\circ$  and  $53 \pm 1.4\%$  at  $120^\circ$ . Neither of these changes were significantly ( $P = 0.205$ ) different. The ratio of variance of contact at  $120^\circ$  versus contact at  $150^\circ$  (variance<sub>120°</sub>/variance<sub>150°</sub>) revealed that variance in percentage contact area decreased as load increased. Areas of contact subjectively appeared to have a higher density on the CT scans as indicated by the pink and green areas (Figures 2 and 3).

## Discussion

The present study revealed that 2 dyes can be used to evaluate articular cartilage contact area under different loads in a single intact joint. The hypothesis that percentage contact area would increase with increased load was confirmed. Results also support the hypothesis that areas of high SCB density are grossly correlated with areas of contact. It appeared that the highest density areas were associated with areas that were in contact under both loads.

The other methods that have been used previously to measure joint contact include pressure measurement systems<sup>13,14</sup> and pressure film.<sup>15,16</sup> The main advantage of the method used in our study was that it allows the joint to remain intact and be tested in the *in vivo* configuration, whereas the other 2 methods require the joint to be opened to insert the sensor, thus disrupting the integrity and normal configuration of the joint and the contribution of joint capsule to normal joint function. In another study,<sup>17</sup> insertion of pressure film changed the contact mechanics of the joint, resulting in measurement errors of 10% to 26%. Therefore, the dye staining method preserves the integrity of the joint environment.

The 2-dye staining technique can be used to evaluate clinically useful methods such as MRI for determination of contact area *in vivo*. An *in vivo* method

would allow for development of a technique to assess the predisposition of a horse to injury before injury occurs. Results of previous studies<sup>18,19</sup> indicate that MRI can be used to assess contact area in the human knee joint. On the basis of the human studies and results of the present study, an MRI-compatible loading jig has been developed and is being used to investigate MRI as a clinically useful method for determining contact area in the equine MCP.

Conformation (either whole-limb conformation or geometric features of bone) that influences contact area in a joint can play a role in predisposition to injury. Anderson et al<sup>20</sup> found that in racing Thoroughbreds, an offset carpus and an increase in forelimb pastern length were both risk factors for musculoskeletal problems in the forelimb. Therefore, having a method to evaluate contact area under different loads within a single limb will be useful in assessing how conformational differences affecting contact area can lead to SCB density patterns that may predispose a horse to injury, whereas another horse in similar circumstances, but with a different conformation, can be unaffected.

Contact area increased under greater load, leading to the conclusion that areas that are not normally loaded in low-load conditions, such as walking or standing, can be subjected to a great degree of stress during impact loading such as during galloping. Brama et al<sup>9</sup> also found that the contact area of the proximal phalanx was positively correlated with the applied load. Even though those authors used force and the angle for joint positioning was used in the present study, the results for the proximal phalanx contact area were similar. Brama et al<sup>9</sup> found that during stance, which they defined as 1,800 N, 63% of the proximal phalanx was in contact with the distal condyle of MC III and during gallop, defined as 10,500 N, they found that 87% was in contact. Results of the present study indicated that 67% and 87% of the proximal phalanx was in contact during stance and gallop, respectively. Brama et al<sup>9</sup> only evaluated the proximal phalanx and did not include values for the proximal sesamoid bones or the distal condyle of MC III. The increased stress and change in loading patterns can lead to bone adaptation that may not always be favorable.<sup>6,21,22</sup> The density of the SCB as determined via CT can give some degree of insight into the adaptation of the bone to the loading; that is, it was found in this study that areas in contact at both loads subjectively appeared to have higher density.

Results of the present study also suggested that the proximal sesamoid bones may account for more of the contact on the distal condyle of MC III as the load increases ( $42\%$  at  $150^\circ$  and  $46\%$  at  $120^\circ$ ), although the difference was not significant ( $P = 0.205$ ). Although the sample size was small and power of the study was low, results might suggest that the proximal sesamoid bones absorb more of the force over a smaller area, compared with the proximal phalanx, and might indicate a possible explanation for the greater frequency of injury of the proximal sesamoid bones, compared with the proximal phalanx. Statistical calculations of the data in the present study indicated that a sample size of 40 would be required for 80% power. Refining the method or the use of another method to decrease the SD may prove

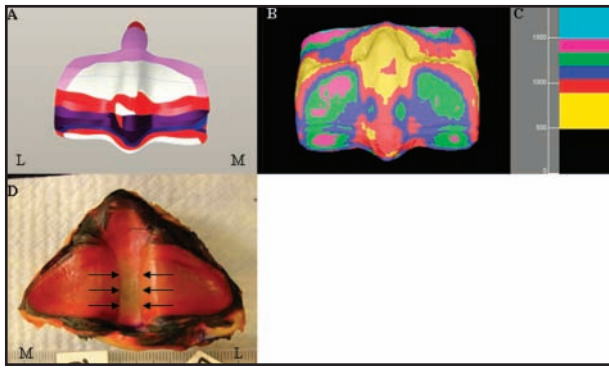


Figure 3—Comparison of a model and 3-dimensional rendering of a CT scan of the MC III in a horse and photograph of the corresponding proximal sesamoid bones. A—Three-dimensional computer model of the palmar surface of the distal condyle of MC III revealing contact area at 150° and 120°. B—Corresponding 3-dimensional rendering of the CT scan revealing SCB density pattern. C—Color scale for CT data with numbers in Hounsfield units. D—Photograph of the proximal sesamoid bones. Notice that there is no staining (arrows) in the area of the intersesamoid ligament, which indicates that there was contact at both loads. See Figure 2 for color scheme.

useful in minimizing the sample size required to detect a significant change in the contact on the distal condyle of MC III by the proximal sesamoid bones, compared with contact by the proximal phalanx.

A subjective comparison of the 3-dimensional computer model of the contact area and the CT scan of the density patterns indicated that areas of contact may be associated with higher SCB density. However, there were areas where there was contact indicated in the model, but those areas correlated with lower density, especially along the sagittal ridge of the condyle. The area on the sagittal ridge is where the intersesamoid ligament contacts the bone. Eckstein et al<sup>23</sup> found that both the geometric joint configuration and the loading conditions influence the SCB density pattern. In their study, cartilage with a higher modulus (stiffer cartilage) resulted in a higher overall density, whereas less stiff cartilage resulted in a lower overall density. The modulus of bone ranges from 3.3 to 17 GPa (cortical) and 0.76 to 10 GPa (trabecular),<sup>24</sup> and the modulus of ligament ranges from 0.011 to 0.332 GPa,<sup>25</sup> depending on orientation and type of testing. This indicates that it would be expected that areas that are in contact with the intersesamoid ligament, a less stiff material, would have a lower overall density than the areas in contact with bone, which is a minimum of 2 times as stiff. Although the dye staining technique does not require the disruption of the joint, it also does not allow for distinction between the degrees of loading, as do methods such as pressure film and pressure measurement systems. Dye staining merely indicates that there is contact in a given area above a certain threshold of loading. However, it would be beneficial to know the stress distribution under different loads and how this relates to the density pattern. Finite element modeling coupled with CT, MRI, or both, may prove to be a non-invasive, clinically useful method of determining this information.

The comparison between the 3-dimensional computer model and the CT scan was subjective, and a

quantitative method is needed. In future studies, the use of a triad would be beneficial in this aspect, allowing for 3-dimensional localization of bones and reference to geometric features of bone. The triad would attach to the MC III near the MCP. The CT scan would be done so that the triad is visible in the image without interfering with areas of interest. The position of the triad would then be modeled in the digitization and modeling step. This would allow the triad in the CT model and the computer model to be registered together which in turn would align the CT scan, revealing the density pattern, with the computer model, revealing the contact area.

Use of the 2-dye staining technique followed by determination of the stress distribution with pressure-film or a pressure-measurement system would be ideal. Combining this with a quantitative method of registering the contact area with the SCB density pattern would allow for development of more complex models. A finite element model could be created with this information, allowing for the manipulation of variables such as applied load and bone geometric features and observation of the resulting changes in SCB density patterns. This can help provide insight into geometric variables and specific loading patterns that may predispose some horses to injury.

- a. Drum MG. *Computed tomographic characterization of the equine third metacarpal bone*. PhD dissertation, Department of Clinical Sciences, College of Veterinary Medicine and Biomedical Sciences, Colorado State University, Fort Collins, Colo, 2006.
- b. Picker PQ 2000, Universal Medical System, Bedford Hills, NY.
- c. OsteoApp, Orthopaedic Research Center, Colorado State University, Fort Collins, Colo.
- d. IDL, version 5.4, Research Systems Inc, Boulder, Colo.
- e. Dyna-Cast, Kindt Collins Co LLC, Cleveland, Ohio.
- f. MTS model 819.1, MTS Systems Corp, Eden Prairie, Minn.
- g. MicroScribe G2, Immersion Corp, San Jose, Calif. Available at: [www.immersion.com/digitizer/](http://www.immersion.com/digitizer/). Accessed December 26, 2006.
- h. ProEngineer, PTC, version 2.0, Needham, Mass. Available at: [www.ptc.com/appserver/mkt/products/home.jsp?k=403](http://www.ptc.com/appserver/mkt/products/home.jsp?k=403). Accessed Dec 26, 2006.

## References

1. Caron JP, Genovese RL. Principles and practices of joint disease treatment. In: Ross RW, Dyson SJ, eds. *Diagnosis and management of lameness in the horse*. Philadelphia: WB Saunders Co, 2003;746–763.
2. Johnson BJ, Stover SM, Daft BM, et al. Causes of death in racehorses over a 2 year period. *Equine Vet J* 1994;26:327–330.
3. Peloso JG, Mundy GD, Cohen ND. Prevalence of, and factors associated with, musculoskeletal racing injuries of Thoroughbreds. *J Am Vet Med Assoc* 1994;204:620–626.
4. McKee SL. An update on racing fatalities in the UK. *Equine Vet Educ* 1995;7:202–204.
5. Riggs CM. Fractures—a preventable hazard of racing Thoroughbreds? *Vet J* 2002;163:19–29.
6. Norrdin RW, Kawcak CE, Capwell BA, et al. Subchondral bone failure in an equine model of overload arthrosis. *Bone* 1998;22:133–139.
7. Eckstein F, Müller-Gerbl M, Steinlechner M, et al. Subchondral bone density in the human elbow assessed by computed tomography osteoabsorptiometry: a reflection of the loading history of the joint surfaces. *J Orthop Res* 1995;13:268–278.
8. Colahan P, Turner TA, Poulos P, et al. Mechanical functions and sources of injury in the fetlock and carpus. In *Proceedings*. 33rd Annu Meet Am Assoc Equine Pract 1987;33:689–699.

9. Brama PAJ, Karssenberg D, Barneveld A, et al. Contact areas and pressure distribution on the proximal articular surface of the proximal phalanx under sagittal plane loading. *Equine Vet J* 2001;33:26–32.
10. McGuigan MP, Wilson AM. The effect of gait and digital flexor muscle activation on limb compliance in the forelimb of the horse *Equus caballus*. *J Exp Biol* 2003;206:1325–1336.
11. Powers CM, Chen YJ, Scherl I, et al. The influence of patellofemoral joint contact geometry on the modeling of three dimensional patellofemoral joint forces. *J Biomech* 2006;39:2783–2791.
12. Ranga A, Mongrain R, Galaz RM, et al. Large-displacement 3D structural analysis of an aortic valve model with nonlinear material properties. *J Med Eng Technol* 2004;28:95–103.
13. Svoboda SJ, McHale K, Belkoff SM, et al. The effects of tibial malrotation on the biomechanics of the tibiotalar joint. *Foot Ankle Int* 2002;23:102–106.
14. Greis PE, Scuderi MG, Mohr RA, et al. Glenohumeral articular contact areas and pressures following labral and osseous injury to the anteroinferior quadrant of the glenoid. *J Shoulder Elbow Surg* 2002;11:442–451.
15. Earll M, Wayne J, Brodrick C, et al. Contribution of the deltoid ligament to ankle joint contact characteristics: a cadaver study. *Foot Ankle Int* 1996;17:317–324.
16. Clark AL, Herzog W, Leonard TR. Contact area and pressure distribution in the feline patellofemoral joint under physiologically meaningful loading conditions. *J Biomech* 2002;35:53–60.
17. Wu JZ, Herzog W, Epstein M. Effects of inserting a pressensor film into articular joints on the actual contact mechanics. *J Biomech Eng* 1998;120:655–659.
18. Patel V, Hall K, Ries M, et al. A three-dimensional MRI analysis of knee kinematics. *J Orthop Res* 2004;22:283–292.
19. Besier TF, Draper CE, Gold GE, et al. Patellofemoral joint contact area increases with knee flexion and weight-bearing. *J Orthop Res* 2005;23:345–350.
20. Anderson TM, McIlwraith CW, Douay P. The role of conformation in musculoskeletal problems in the racing Thoroughbred. *Equine Vet J* 2004;36:571–575.
21. Wohl GR, Boyd SK, Judex S, et al. Functional adaptation of bone to exercise and injury. *J Sci Med Sport* 2000;3:313–324.
22. Pool RR, Meagher DM. Pathological findings and pathogenesis of racetrack injuries. *Vet Clin North Am Equine Pract* 1990;6:1–30.
23. Eckstein F, Jacobs CR, Merz BR. Mechanobiological adaptation of subchondral bone as a function of joint incongruity and loading. *Med Eng Phys* 1997;19:720–728.
24. Huiskes R, Van Rietbergen B. Biomechanics of bone. In: Mow VC, Huiskes R, eds. *Basic orthopaedic biomechanics and mechano-biology*. 3rd ed. Lippincott Williams & Wilkins, 2005;123–179.
25. Woo SLY, Lee TQ, Abramowitch SD, et al. Structure and function of ligaments and tendons. In: Mow VC, Huiskes R, eds. *Basic orthopaedic biomechanics and mechano-biology*. 3rd ed. Lippincott Williams & Wilkins, 2005;301–342.